Journal of Applied Sciences, 2010
ISSN 1812-5654

Preservation of Biogenerated Mixed Facies: A Case Study from the Neoproterozoic Villa Mónica Formation, Sierra La Juanita, Tandilia, Argentina

[1]P.E. Zalba, [2]M. Manassero, [3]M.E. Morosi and [4]M.S. Conconi
[1]Comisión de Investigaciones Científicas, Provincia de Buenos Aires-CETMIC,
Adjunct Research Fellow, School of Geosciences,
Monash University, Melbourne, Australia
[2]CONICET-Centro de Investigaciones Geológicas,
Facultad de Ciencias Naturales y Museo de La Plata, Argentina
[3]Comisión de Investigaciones Científicas Provincia de Buenos Aires-CETMIC,
Facultad de Ciencias Naturales y Museo de La Plata, Argentina
[4]Comisión de Investigaciones Científicas Provincia de Buenos Aires-CETMIC,
Facultad de Ingeniería de La Plata, Argentina

Abstract: The aim of this contribution was to show through field work and mineralogical microtextural studies a complex history of weathering and diagenesis in the Villa Mónica Formation, the most ancient Neoproterozoic unit of the Tandilia System and to present a proposal of a paragenetic sequence. This unit also shows microbially induced structures described here for the first time. At the Estancia La Siempre Verde, La Placeres and Don Camilo quarries, Sierra La Juanita, near Barker locality, the Villa Mónica Formation is composed of carbonate facies, classically defined for more than 40 years as siliciclastic facies and of reinterpreted mixed facies: carbonate/siliciclastic and heterolithic respectively, both bearing biosignatures. The carbonates are represented by well-preserved columnar head stromatolite boundstones and by laminar microbial mat deposits. Both of them were the host rocks - identified here for the first time - of individual or random aggregates of pyramidal quartz megacrystals and they were later dolomitized, silicified, illitized and hematized. The siliciclastics are composed of quartz grains trapped within both the stromatolites and the microbial mats, of illitic siltstones and claystones and of quartzitic sandstones. Illuviation processes transported cutans to lower horizons. Syndiagenesis involved dolomitization and silicification while burial diagenesis produced pressure-solution effects by overburden and neoformation of minerals: diagenetic illite with rutile needles, among others. Compressive movements from the SW, responsible for basin inversion: telodiagenesis (uplift, fracturing, folding and introduction of meteoric fluids), affected the Villa Mónica Formation with neoformation/transformation of minerals: kaolinite, halloysite and smectite, development of slickensides (stress cutans) and ferriargillans, hydration, dedolomitization and calcification.

Key words: Neoproterozoic, biogenerated rocks, weathering, diagenesis, paragenetic sequence

INTRODUCTION

There are several previous contributions describing the sedimentary cover of the Tandilia system within the Barker area, Sierra La Juanita (Schauer and Venier, 1967; Cingolani *et al*., 1985; Manassero, 1986; Iñíguez *et al*., 1989; Alló *et al*., 1996; Alló, 2001; Alló and Dominguez, 2002; López Escobar *et al*., 2002; Poiré and Spalletti, 2005; López Escobar, 2006; Zalba *et al*., 2007a; Gómez Peral, 2008). But here, for the first time, mixed carbonate/siliciclastic facies were recognized in microscopic scale in the Villa Mónica Formation, overlying basal quartzite deposits known in the geological literature as the Cuarcitas Inferiores (and which are beyond the scope of this study). Besides, reinterpreted heterolithic facies replaced the previously named *Psamopelites* defined by Poiré and Iñíguez (1984) and considered by these authors as part of the overlying Cerro Largo Formation (Poiré, 1993).

The Neoproterozoic Villa Mónica Formation is the oldest sedimentary unit of the Tandilia System unconformably overlying the basement rocks (Fig. 1, 2). Originally defined by Poiré (1987) in the Sierras Bayas region (stratotype area) as a 52 m thick sedimentary

Corresponding Author: Patricia Eugenia Zalba, Camino Centenario y 506, M.B. Gonnet (1897), Provincia de Buenos Aires, Argentina Tel/Fax: 00542214248725

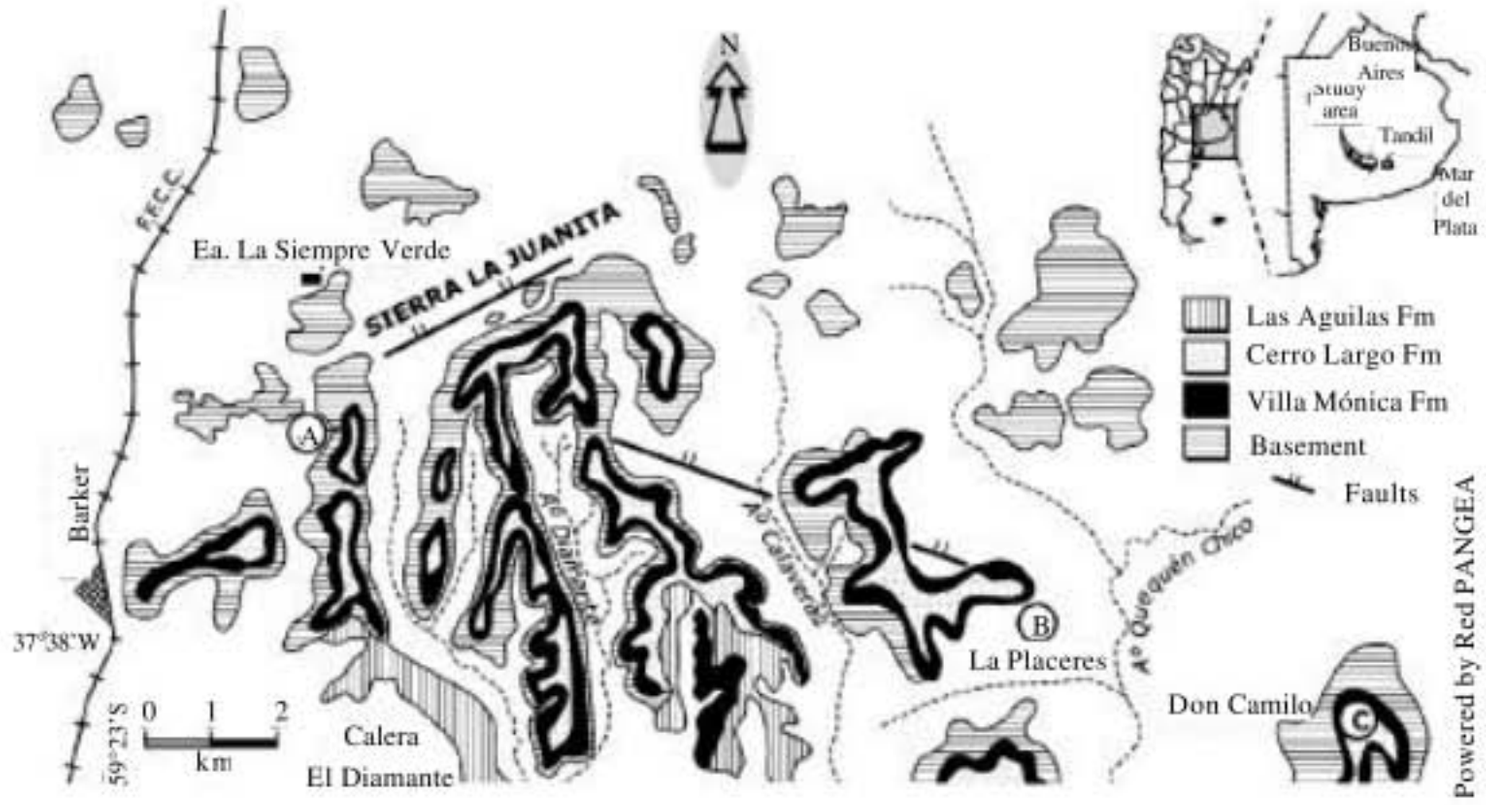

Fig. 1: Geological map of the study area Tandilia system. A, B and C: location of stratigraphic sections from which an integrated section is presented

Age \ Area	Sierras Bayas		Barker		Sedimentary Cycles
Early Ordovician			Balcarce Fm. (quartzite)		Batán
Neo Proterozoic	Cerro Negro Fm. (claystone, marl and limestone)		Las Aguilas Fm. (claystone, marl and limestone)		La Providencia
	Sierras Bayas Group	Loma Negra Fm. (limestone)	Sierras Bayas Group	Loma Negra Fm. (limestone)	Villa Fortabat
		Olavarría Fm. (claystone)		Las Aguilas Fm.(?) (breccia, claystone and quartzite)	Diamante
		Cerro Largo Fm. (quartzite)		Cerro Largo Fm. (quartzite)	Malegni
		Villa Mónica Fm. (dolomite, claystone and quartzite)		Villa Mónica Fm. (dolomite, claystone and quartzite)	Tofoletti
Paleo Proterozoic	Complejo Buenos Aires (granitoids)				

Fig. 2: Stratigraphic scheme of Tandilia for the two areas where the Villa Mónica Formation outcrops: Sierras Bayas (stratotype area) and Sierra La Juanita

succession and bound by unconformities at the base and top, it is represented, in this region, located 100 km NW from the study area, by two sedimentary facies associations: (1) quartz-arkosic arenites (16 m) at the base (the Cuarcitas Inferiores) and (2) biogenic dolomites (36 m) with columnar or laminar shallow marine stromatolites. Poiré (1993) included red, laminated claystone and calcipelite deposits at the top of the unit.

In the Barker study area within the Sierra La Juanita, the most important outcrops of this unit were studied at Estancia La Siempre Verde, La Placeres and Don Camilo quarries, along a NW-SE transect which extends for more than 20 km (Fig. 1). Yet, the deposits of the Villa Mónica Formation at the Sierra La Juanita, Barker area, are much thinner and the exposures are not as good as in the stratotype area.

The Villa Mónica Formation was considered to be of Riphean age, (upper Proterozoic) based on stromatolites (Poiré, 1993) and also on Rb-Sr dating of clay deposits associated with dolomites at the Sierras Bayas area, giving an age of 793±32 Ma for the diagenesis of the unit (Cingolani and Bonhomme, 1982). Nevertheless, according to Gaucher (2005) while stromatolite association suggests an early Neoproterozoic age, the similarity of acritarch assemblages preserved throughout the Sierras Bayas Group suggests that there is a short time hiatus between the two basal units of the Sierras Bayas Group: the Villa

Mónica Formation and the overlying Cerro Largo Formation, raising the possibility of the Villa Mónica Formation being of Ediacaran age.

Microtextural observations have proved to be crucial in the recognition of biogenic fabrics due to microbial activity. A complex history of weathering and diagenesis has left its imprint in the sediments leading to the present status of the rocks. Where morphology could not be of help in the recognition of biogenic relics, structures certainly were and diagenetic processes (e.g., silicification, hematization) also helped in the preservation of diagnostic remains (cellular structures, rhomboedral pseudomorph crystals of quartz after dolomite, crinkled structures) which, otherwise, would probably have been erased from the sedimentary record.

A paragenetic sequence of events is proposed and the influence of the uplift of the Ventania System, located 150 km to the SE, over the geological evolution of Tandilia is considered on the basis of a recent contribution (Zalba *et al*., 2007b).

MATERIALS AND METHODS

This study was conducted between 2006 and 2008. Forty-five thin sections were examined using optical microscopy to determine textural and optical properties as well as the mineral paragenesis. Selected samples were tinted with Alizarin red and observed by optical microscopy on uncovered thin sections. A Philips 505 scanning electron microscope was used to examine textural features, morphology and the sequence of mineral formation. X-ray diffraction analyses were carried out on a Philips 3020 Xpert Pro device equipped with an Xcelerator detector, at 40 kV and 20 mA, with Cu Kα radiation and Ni filter. Clay minerals were analyzed on randomly oriented powders for routine analysis (<2 μm size fraction). Determination of interstratified clay minerals (illite-smectite) was achieved using Srodoń (1984) method. Quantitative X-ray diffraction analyses were carried out using the Rietveld method (Rietveld, 1969). In the identification of micas on total sample the presence of diffraction lines corresponding to muscovite $2M_1$ and the two characteristic lines of the polytype $1M_1$ (-112 and 112) in 3.66 and 3.07 Amstrong, respectively were observed. That is why in the refinement by the Rietveld method for the quantification of the samples both muscovite polytypes were considered. When the content of micas did not exceed 40% or when they exhibited poor crystallinity, polytypes were not identified. Crystallographic data of polytype $2M_1$ were taken from Liang and Hawthorne (1996) and those of polytype $1M_1$ were obtained from Plançon *et al.* (1985).

INTEGRATED STRATIGRAPHIC SECTION

This contribution integrates the stratigraphic analysis of carbonate (C) and mixed (carbonate/siliciclastic: C/S and heterolithic: H) facies of the Villa Mónica Formation, Sierra La Juanita, with new material collected from three geologic sites. The studied outcrops: Estancia La Siempre Verde, La Placeres and Don Camilo, are located 4.5 km. East, 14 km. East and 20 km SE, respectively from Barker (Fig. 1). The integrated stratigraphic section with all the sedimentary features found in the studied areas is presented in Fig. 3.

From field observations, the C facies are represented by head, brownish, well-preserved columnar stromatolite dolostones. They are well-exposed at the Estancia La Siempre Verde, whereas only the top of these deposits outcrops at La Placeres quarry and, at Don Camilo quarry, are not exposed. These rocks form bioherms (mounds) up to 4 m high (Fig. 4a), containing scarce sandy siliceous trapped sediments and forming cavernous structures. The mounds show distinctive columnar stromatolite structures (Fig. 4b) and are crossed by fractures, filled with silica or with calcite cement. Random aggregates of pyramidal quartz megacrystals, up to 20 cm long and 10 cm wide, are found growing in fenestral cavities in the dolostones (Fig. 4c, d).

The C/S facies show up to 6 m thick banded, brownish to yellowish, weathered dolostones with intercalated siliciclastics, the latter represented by greenish, laminated clay, silt or sand beds (Fig. 5a). The weathered dolostones also bear loose, individual or random aggregates of pyramidal quartz megacrystals, ranging from approximately 10 cm to 1 cm long and 5 cm to few mm wide (Fig. 5b). Complex fracture-network systems, filled with reddish clays showing slickensides, cut the deposits in several directions at different levels (Fig. 5c) and also have spread along sedimentary discontinuities (e.g., between the C/S and the upper H facies).

The H facies, with a maximum thickness of 2 m, consist of a thickening and coarsening upwards, cross-laminated and rippled lenticular quartzites with intercalated greenish clay deposits. (Fig. 6a, b).

A NW-SE normal fault cross the front of the La Siempre Verde quarry and extends towards the La Placeres and Don Camilo quarries. Flexuration, fracturing and local brecciation of the deposits are clearly observed in the front quarries.

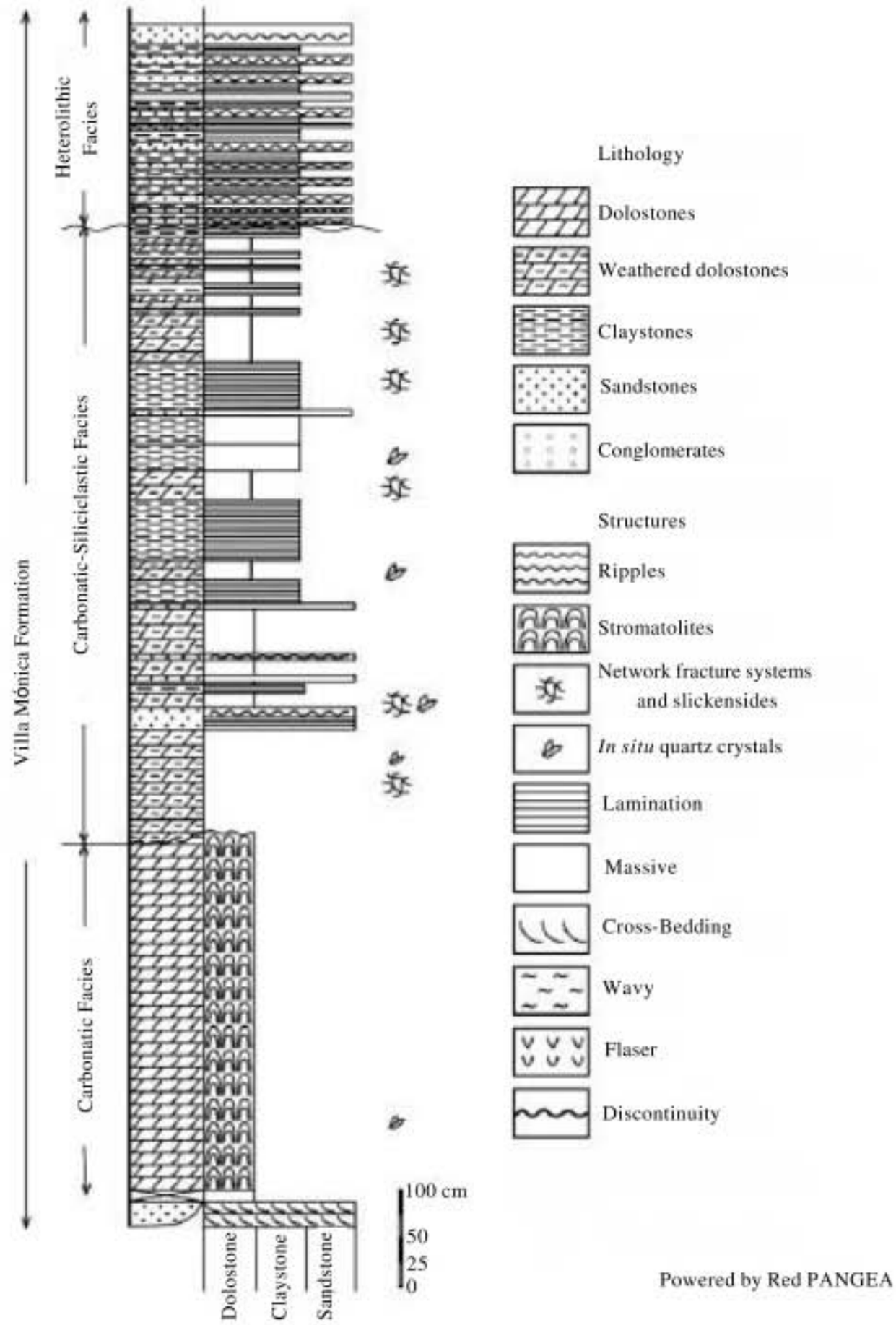

Fig. 3: Integrated stratigraphic section of the Villa Mónica Formation, Sierra La Juanita, based on stratigraphic sections A, B and C

RESULTS

Petrography and mineralogy

Carbonate facies (C): The fabric is represented by bimodal rhombohedric carbonate crystals of <340 and <250 μm in size, respectively (Fig. 7a, b). Contacts between grains are planar. Staining with Alizarin red shows that dolomitization was complete and that sparry calcite is present in fractures and in very small cavities (Fig. 7c). The rocks show typical stromatolite lamination (Fig. 7d), which attests to the precipitation of calcite from algae activity. On the basis of Dunham (1962) classification, these rocks are columnar boundstones.

Epitaxial calcite rims on dolomite crystals are observed, being even and uniform in thickness (45 μm) and with lengths of 300 μm. Stained calcite rims (Fig.7e darker in the photograph) are easily distinguishable from dolomite crystals. Ferric oxides and hydroxides are represented by hematite and abundant goethite, with minor ferric oxides also present in fractures and surrounding dolomite crystals, having precipitated previous to the epitaxial calcite rims.

The dolostones show silicification processes (Fig. 7f). Quartz is present as individual crystals or as random aggregates of megacrystals, which have grown in major cavities, in fractures or as pseudomorphs after

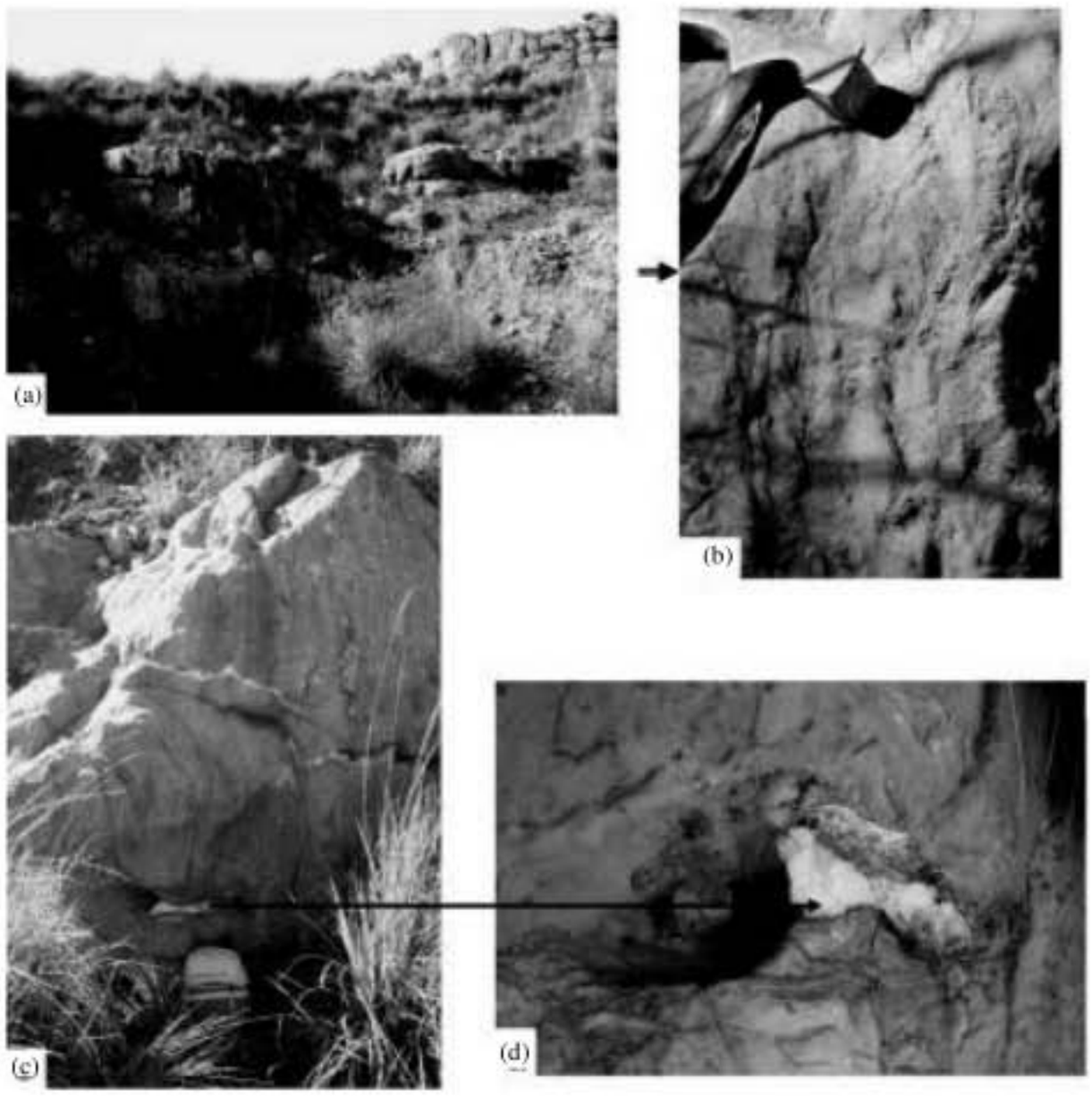

Fig. 4: Estancia La Siempre Verde quarry, Sierra La Juanita. (a) General view of the stromatolitic boundstones, (b) detail columnar stromatolitic structures, (c) cavities in the stromatolitic boundstones with random aggregates of quartz megacrystals and (d) close up of quartz megacrystals

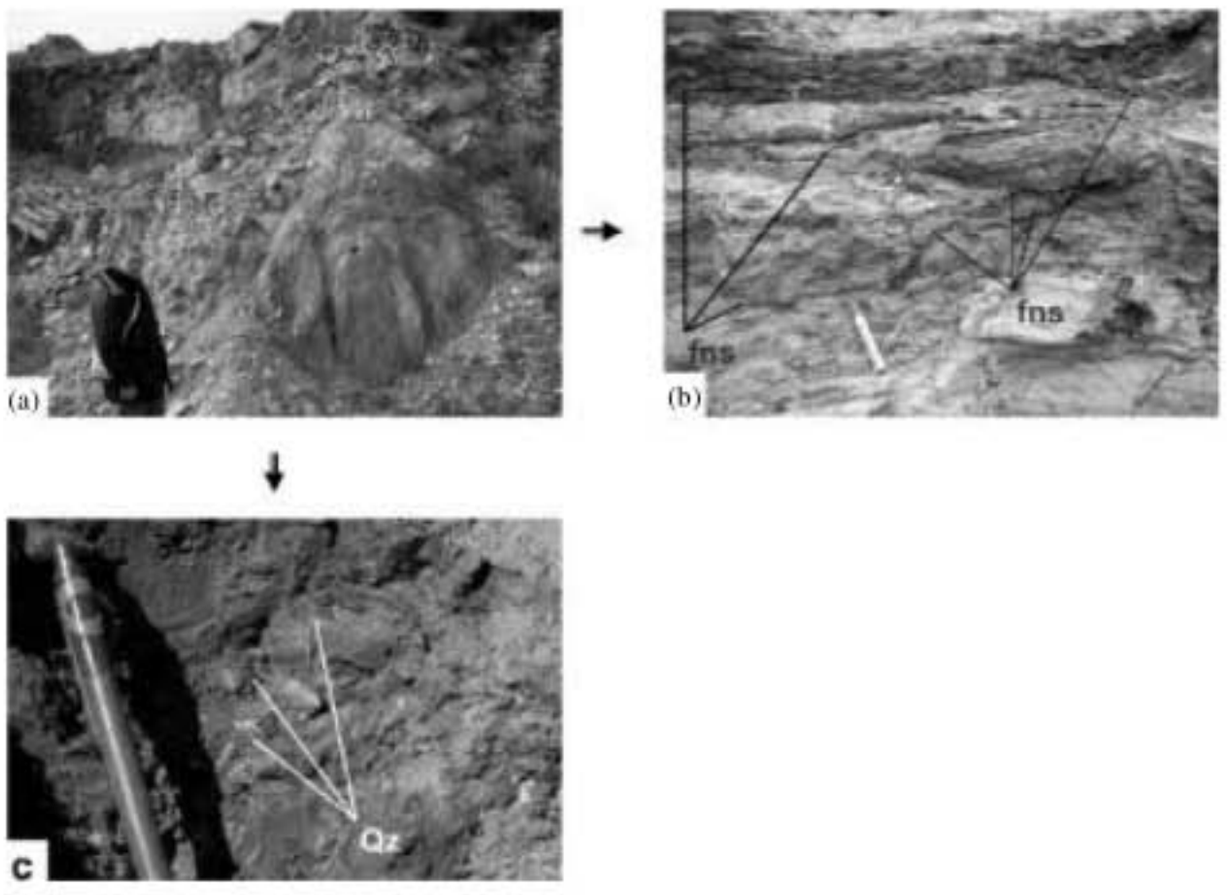

Fig. 5: Estancia La Siempre Verde quarry. (a) View of the weathered laminar dolostones: boundstones, with centimeter to millimeter-thick intercalations of greenish, laminated clays, silt or sand beds, (b) a complex fracture network system (fns) filled with reddish clays, with slickensides cutting the weathered laminar dolostones at all levels and (c) individual quartz megacrystals dispersed in the weathered laminar dolostones

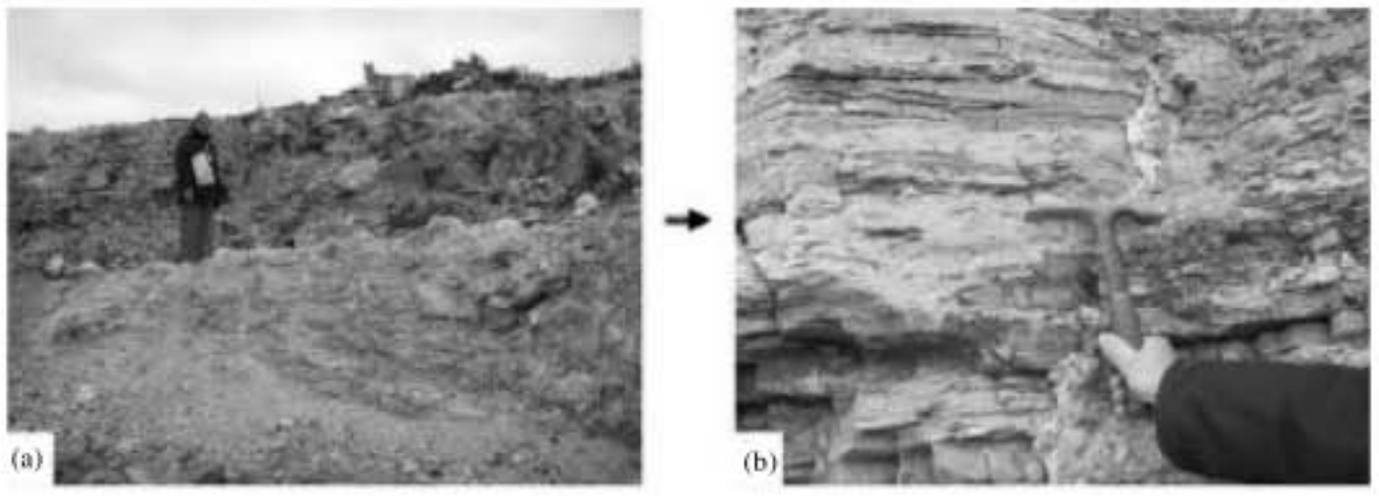

Fig. 6: Don Camilo quarry. (a) View of the heterolithic Facies and (b) Detail

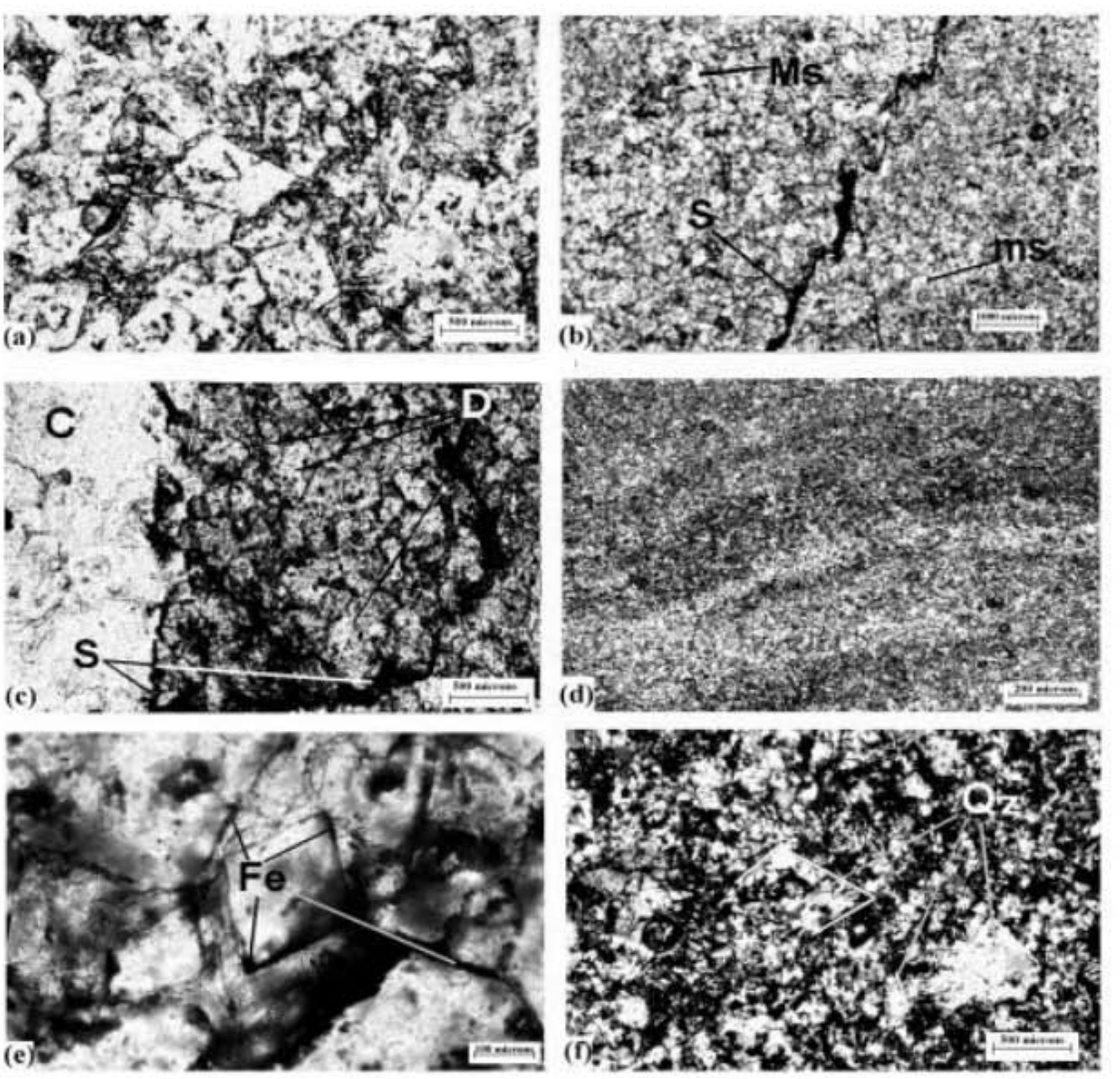

Fig. 7: Thin sections of C Facies. La Placeres quarry. (a) Bimodal dolomitized rhombohedric carbonate crystals. (b) Estancia La Siempre Verde quarry Idem. Ms: macroesparite. ms: microesparite. Sample stained with Alizarin-red. S: stylolite filled with ferric oxides. (c) Staining with Alizarin-red shows that dolomitization was complete, (D: dolomite, dark part of the photograph). Calcite fills fractures (C: white part of the photograph). (d) Banded structure (stromatolites). (e) Epitaxial calcite rims on dolomite crystals (arrow). Fe: ferric oxides. Sample stained with Alizarin-red. (f) La Placeres quarry. Quartz pseudomorphous after dolomite rhombohedric crystals. Quartz: Qz. (X nicols)

Table 1: Quantitative X-ray diffraction analyses on total samples. (Rietveld method)

Sample	Quartz	Kaolinite	Illite	Tryd.	Smectite	Goethite	Dolo.	Calcite	Rutile	Anatase
Estancia La Siempre Verde quarry										
6	-	81	19		-	-	-	-	-	-
5	4	40	36		-	17	-	-	-	3
4	28	10	15		n.d.	47	-	-	-	-
3	19	-	$1M_1$: 15 $2M_1$: 61		2	-	-	1	3	-
2	24	n.d.	$1M_1$: 19 $2M_1$: 32			25	-	-	-	-
1	39	n.d.	41		-	20	-	-	-	-
0	10		24	46		20				
00	5	-	5	-		3	79	8	-	-

Sample	Quartz	Kaolinite	Illite	Smectite	Goethite	Rutile	Anatase
La Placeres quarry							
30	10	73	13	-	4	-	-
29	42	4	38	-	16	-	-
28	-	17	$1M_1$: 16 $2M_1$: 40	13	2	2	-
27	9	56	21	6	8	-	-
26	-	8	$1M_1$: 16 $2M_1$: 56	16	2	2	-
25	20	54	16	10	-	-	
24	-	32	$1M_1$: 9 $2M_1$: 41	13	3	-	1
23	19	22	32	15	11	-	1
22	37	8	36	6	13	-	-
21	24	12	$1M_1$: 15 $2M_1$: 33	11	5	-	-
20	14	36	29	-	21	-	-
19	30	5	$1M_1$: 20 $2M_1$: 31	-	14	-	-
18	55	2	23	-	20	-	-

Sample	Quartz	Kaolinite	Illite	Smectite	Goethite	Rutile	Anatase
Don Camilo quarry							
14	37		$1M_1$: 19 $2M_1$: 36		4	4	
13	26	2	$1M_1$: 27 $2M_1$: 39	2	20	4	-
12	18	-	$1M_1$: 16 $2M_1$: 27	-	30	1	-
11	17	7	$1M_1$: 8 $2M_1$: 37	3	27	1	-
10	49	-	24	-	27	-	-
9	38	1	$1M_1$: 26 $2M_1$: 34	-	3	1	-
8	-	-	-	-	-	-	-
7	65	4	10	2	19	-	-
6	16	-	10	-	-	-	-
5	29	42	10	2	17	-	-
4	7	2	$1M_1$: 33 $2M_1$: 55		-	3	-
3	6	9	7	13	78	-	-
2	-	3	$1M_1$: 26 $2M_1$: 68	-	-	-	-
1	26	tr	37	-	34	1	1

Values are given in percentages. $1M_1$ and $2M_1$: illite polytypes. nd: Not detected. Absolute error: ±5%. Samples with smectite, poor crystallinity or abundant Fe content may display greater errors

rhombohedric dolomite crystals, also surrounded by hematite and/or goethite. Small cavities and fractures are filled with calcite or with quartz. X-ray diffraction analyses show that they consist of 79% replacement dolomite, quartz and illitic material (I+ISII), with <15% of expanded layers (Table 1, sample 00).

Carbonate/siliciclastic facies (C/S): The carbonates of these facies are represented by relic domal or laminar stromatolite dolostones, where rhombohedric dolomite crystals have lost their continuity and have been completely replaced by illitic material (I+ISII), with less than 15% of expanded layers (Table 1). The illitic clay includes rutile needles, which are 20 to 30 μm long, intersecting to form asterisk-shaped units showing a sagenite-like texture (Fig. 8a). Some of the relic rhombohedric dolomite crystals show silicified cellular structures (Fig. 8b) that could be related to microbial

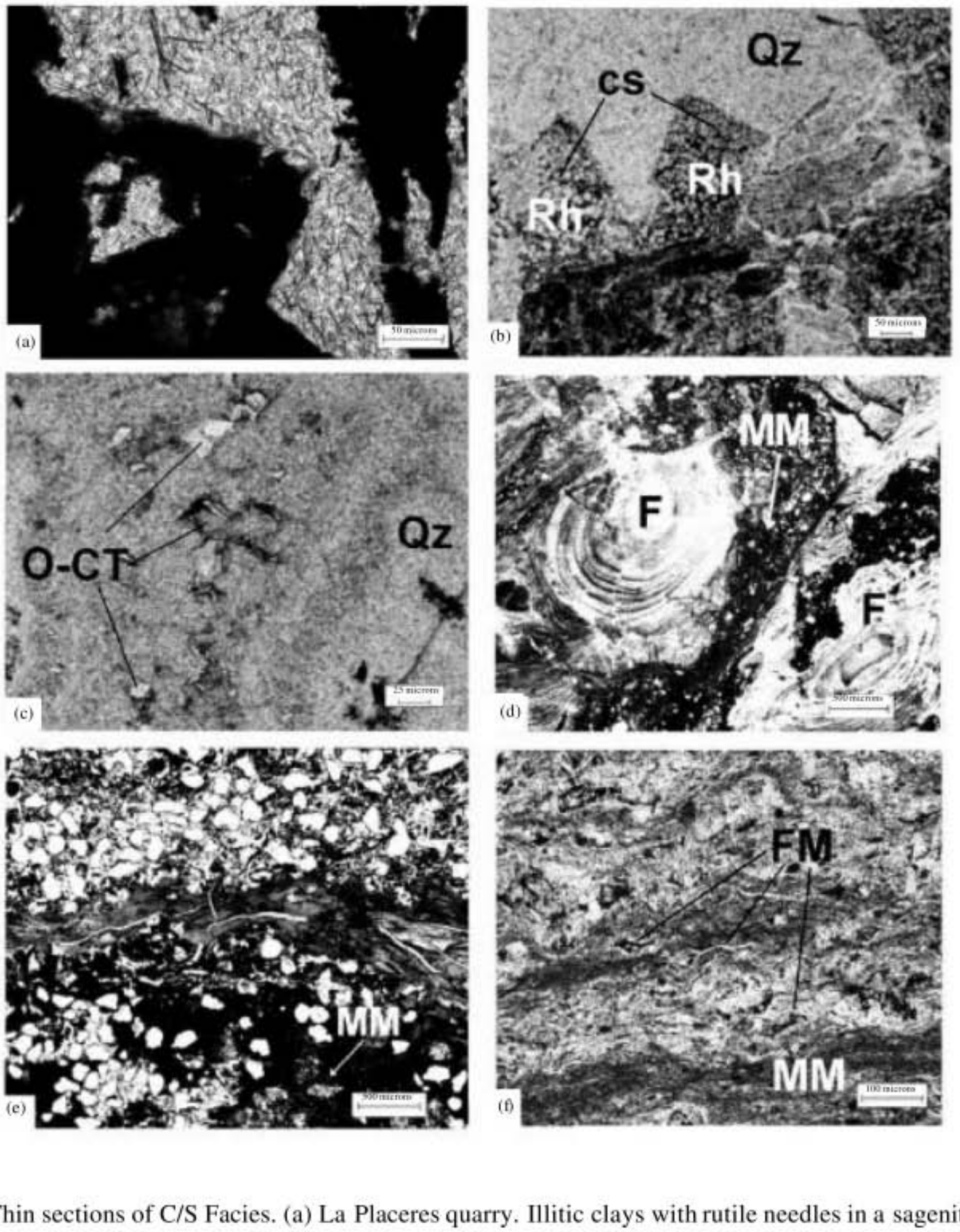

Fig. 8: Thin sections of C/S Facies. (a) La Placeres quarry. Illitic clays with rutile needles in a sagenitic-like texture filling cavities and replacing relic dolomite rhomboedric crystals. (b) Estancia La Siempre Verde quarry. Quartz megacrystals (Qz) include rhombohedric dolomite crystals (Rh) which show cellular structure (cs). (c) Detail. Quartz (Qz) includes opal-CT (O-CT). La Placeres quarry: (d) Ferriargilans (F), some of them with spherical shapes, showing parallel lamination and filling cavities developed among relic microbial mats (in black: MM) with isolated, detrital quartz grains. (e) Fractures filled with ferriargilanes (middle part) crossed by smaller fractures filled with kaolinite. Lower part (in black: MM): relic of microbial mat deposits with detrital quartz grains trapped within. Upper part: siliciclastic deposit with abundant detrital quartz grains floating in an illitic epimatrix and (f) Crinkled dark microbial mat deposits (MM) alternate with illitized carbonate deposits (light color). Several parallel to bedding flexured mica laminae (FM) are seen within the microbial mats

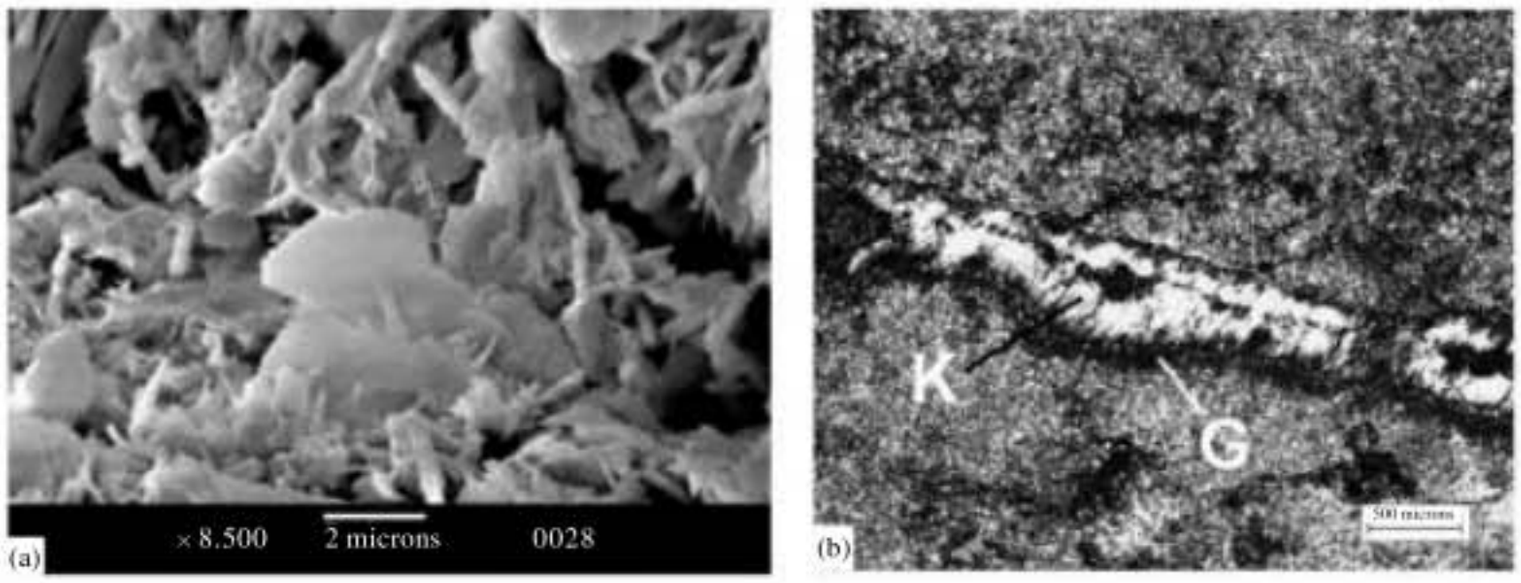

Fig. 9: Micrographs of the C/S Facies. La Placeres quarry: (a) Scanning electron micrograph. Hexagonal plates of kaolinite with tubes of halloysite growing on its surface and (b) Kaolinite cutans (K) filling fractures and surrounded by goethite (G)

activity. Quartz megacrystals (Fig. 8b) have grown in large cavities (fenestral porosity) and, in some cases, include opal-CT (Fig. 8c) identified as trydimite by X-ray diffraction (Table 1, sample 0).

Cavities are large in comparison with the previous lithofacies and goethite is abundant, surrounding replaced dolomite crystals (Fig. 8b). When cavities increase in size they connect with each other and, occasionally, they are filled with quartz megacrystals.

Typical cutans (Brewer, 1960, 1976) are represented by ferriargillans and clay infillings. Ferriargillans show spherical or ellipsoidal shapes, parallel lamination and are rich in ferric hydroxides (goethite), kaolinite and minor smectite, showing orange to yellowish colors. Orientation of the clay laminae produces extinction when parallel to the polarizers (Fig. 8d). Ferriargillans fill cavities developed among relics of the original rhombohedric dolomite crystals, now replaced by illitic material and disrupt black, hematized microbial mat deposits (MM: Fig. 8d). Two types of clay infillings, which block up cavities, were distinguished: (1) brownish kaolinite (Table 1, sample 20), lacking rutile needles and showing a book texture. They are discernible by their interference color from (2) illitic clay (dark grey) which is composed of a mixture of $1M_t$ and $2M_t$ polytypes (Table 1), where $2M_t$ predominates over $1M_t$. Kaolinite, associated with smectite and goethite, fills fractures and micro fractures with different orientations, as have been shown (Fig. 5c) in the field cutting the weathered dolostones at all levels and showing slickensides (stress cutans). The ferriargillans and the original dolomite texture are also cut by micro fractures filled with kaolinite, smectite and goethite. Detrital quartz grains, with overgrowths and undulate extinction, show some orientation within the relic dolostones and also seem to form defined siliciclastic intercalations. The relationships among detrital quartz, ferriargillans, clay infillings, original rhombohedric dolomite texture and fractures are shown in Fig. 8e. In some cases, the ferriargillans have been disrupted and brecciated by the infiltration of kaolinitic clay. In Fig. 8f crinkled dark microbial mat deposits (MM) alternate with illitized carbonate deposits (light color). Flexured micas laminae are clearly observed within the microbial mats.

Scanning electron microscopy shows plates of hexagonal kaolinite and tubes of halloysite developing on the kaolinite surface (Fig. 9a). Kaolinite cutans also fill fractures inclined or parallel to the stromatolitic structure, whereas ferric hydroxides (goethite) coat the fracture walls (Fig. 9b).

The siliciclastics in the C/S facies are represented by silt to clay-sized layers and by minor sand deposits. The fines may show lamination, graded structure and stylolites parallel and inclined to bedding, either filled with clay, sand and/or hematite, the perpendicular stylolites cutting the parallel ones (Fig. 10a).

The quartz sandstones show great compaction, sutured boundaries and concave-convex contacts between grains, undulate extinction, fluid inclusions and dissolution features (Fig. 10b). Deformational features (e.g., folding) are common in these rocks, which show connected cavities filled either with clays or quartz cement. Quartz grains show dissolution effects. Some quartz crystals have also been broken and pulled apart by the introduction of clay, as shown along stylolite surfaces (Fig. 10c). The clay introduced between grains is kaolinite.

As shown by X-ray diffraction, silt to clay-sized beds are composed of predominantly illitic material (I+ISII) with <15% of expanded layers. Quantification of $1M_t$ and $2M_t$ illite polytypes shows that the $2M_t$ polytype predominates over $1M_t$ in the total sample (Table 1). Illitic material bears rutile needles (5 to 30 μm long) arranged in

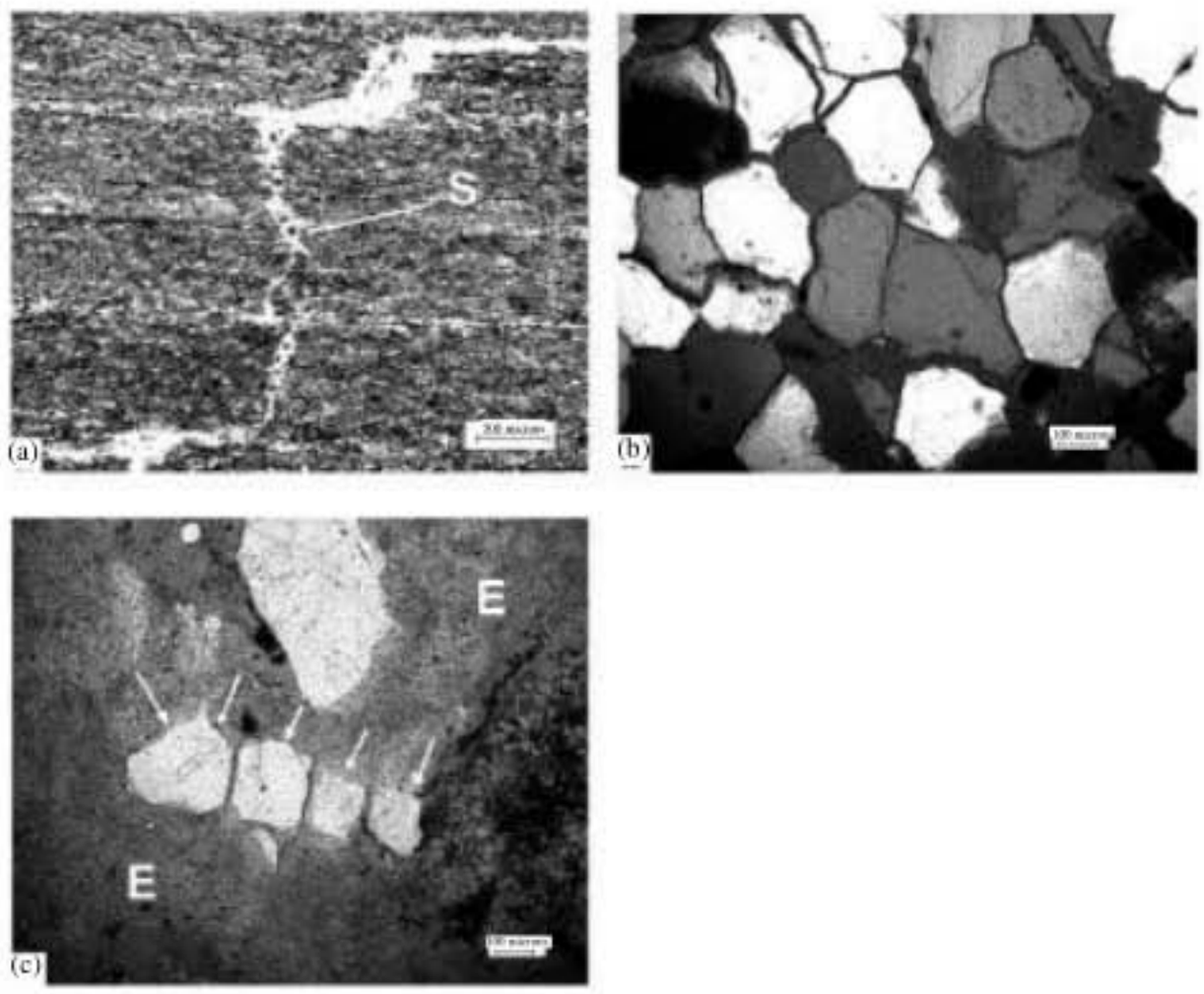

Fig. 10: Thin sections of the C/S Facies. La Siempre Verde quarry: (a) Stylolite (S) perpendicular to bedding cut graded illitic clay levels. Stylolite is filled with detrital material. (b) La Placeres quarry: Quartzite. Detrital quartz grains, with secondary overgrowths, have been broken and pulled-apart by the infiltration of clays (dark rims). X nicols. (c) Dissolutions effects (arrows) due to the development of a stylolite surface on detrital quartz grains, also disrupted by the introduction of epimatrix (E)

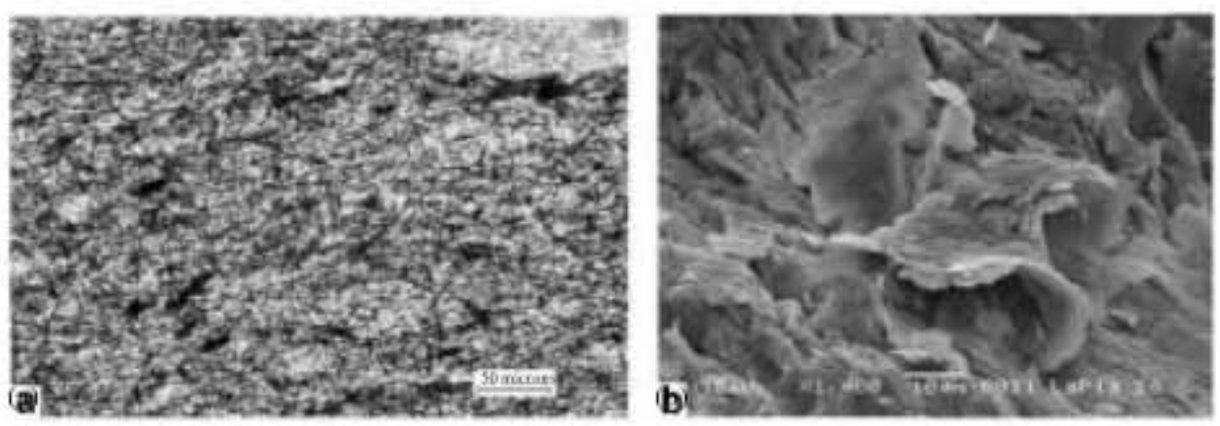

Fig. 11: Micrographs of the C/S Facies. La Siempre Verde quarry: (a) Thin section. Illitic clay ($2M_1$ and $1M_1$ polytypes) bearing rutile needles in a sagenitic-like texture. (b) Scanning electron micrograph of illitic clays showing face-to-face disposition of platelets, certain swirl pattern and rugged borders

a sagenite-like texture (Fig. 11a). Scanning electron microscopy shows the remains of a face-to-face arrangement of the illite, with certain swirl pattern and dissolution features (Fig. 11b). Cavities and fractures parallel to the lamination, are filled with kaolinite, showing a book texture and is surrounded by ferric hydroxides (goethite). Mica flakes are abundant, oriented parallel to the lamination and flexured. Individual cubic pyrite crystals have been completely hematized and disrupt the lamination.

Heterolithic facies (H): These facies, characterized in the field as sandstone/claystone sediments, show in thin sections textural features, such as crinckly laminae and crinkled surface relief on otherwise smooth bedding planes (Fig. 12a). In the same photograph, black, hematized, crinckly laminae with isolated, detrital grains within represent microbial mats.

Quartz sandy deposits show graded structure and the grains float in an illitic epimatrix (Fig. 12b). Finally, at the top of the H facies (Fig. 12c) compact sandstone

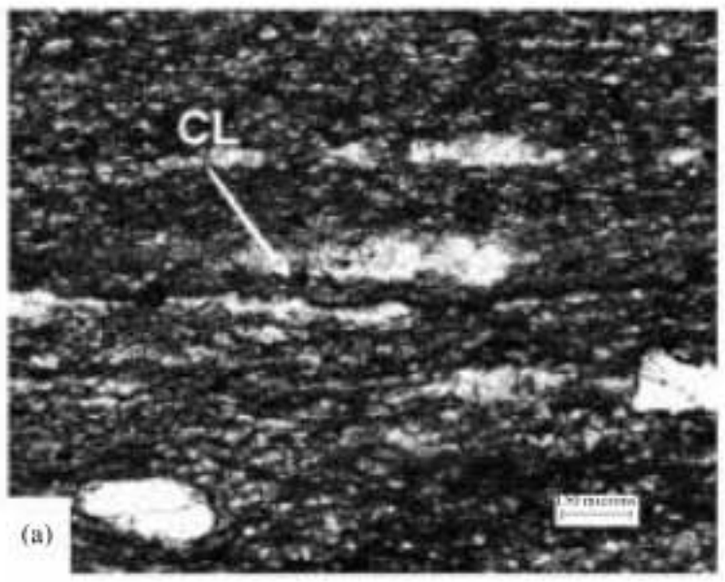

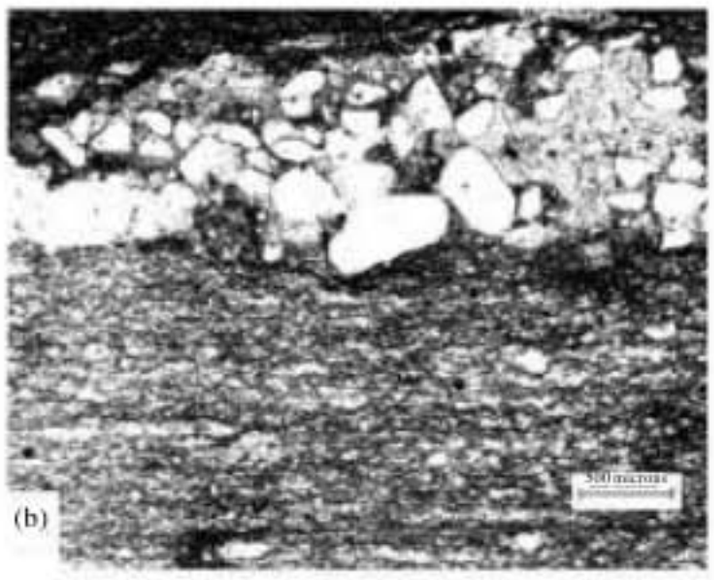

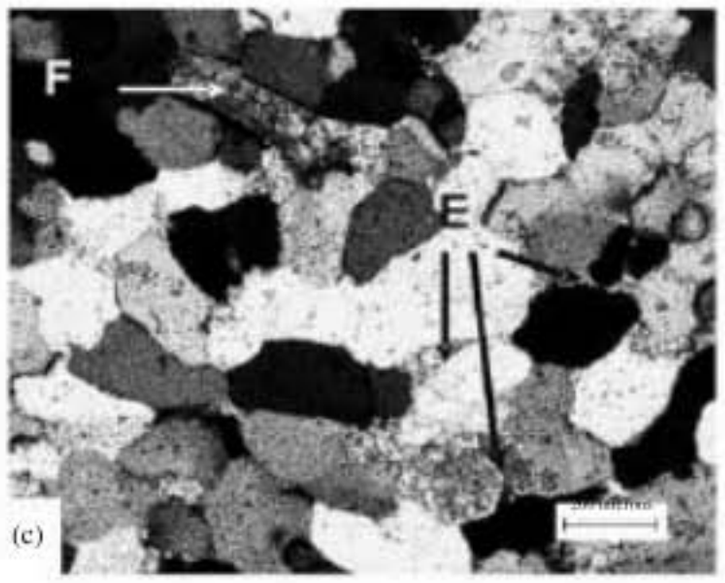

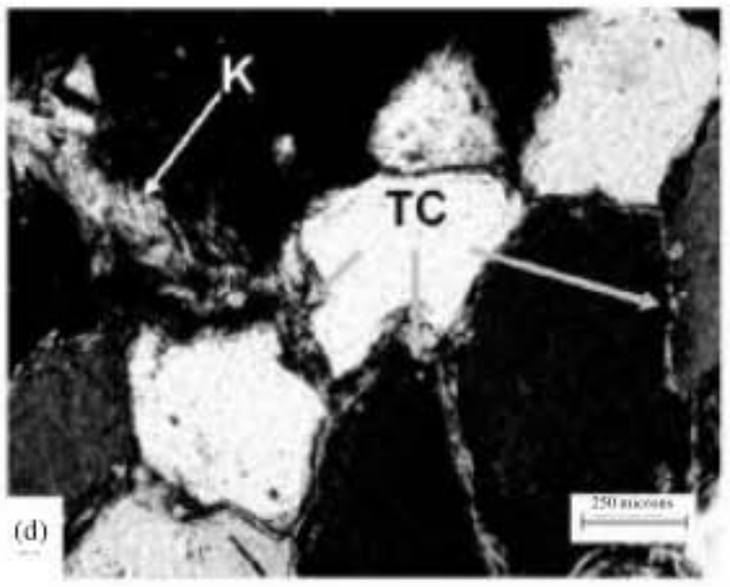

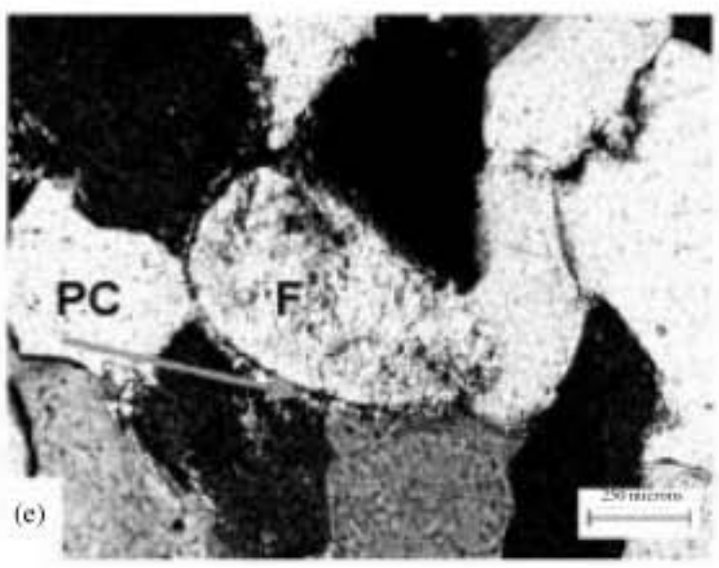

Fig. 12: Thin sections of H Facies. Don Camilo quarry: (a) Hematized microbial mats (dark in the photograph) with crinkly laminae (LC), illitic clay (epimatrix) and isolated detrital quartz grains with their long axis oriented parallel to bedding. (b) Millimetric-scale graded siliciclastic intercalations in microbial mat deposits floating in an epimatrix. (c) Quartzite at the top of the H facies. Quartz grains with secondary overgrowths, sutural contacts between grains (concave-convex contacts). Arrow indicates feldspar altered to illite (F). Illitic epimatrix as tangential clay coatings (E) probably introduced by soft sediment deformation processes. (d) Quartzite at the top of the H facies. Tangential clay coatings (TC) on quartz grains (epimatrix). (e) Quartzite at the top of the H facies. Perpendicular clay coatings (PC) of diagenetic illite on feldspars (F)

layers are composed of well-sorted, rounded quartz grains with secondary overgrowths, fluid inclusions and undulate extinction. Boundaries between quartz grains are sutured (concave-convex contacts). Euhedral feldspars have been altered to illitic material with <15% of expanded layers. Illitic material, together with quartz grains and hematite also fill irregular cavities and intergranular fractures, bearing rutile needles. Kaolinite tangential clay coatings around quartz grains and kaolinite introduced in fractures are clearly observed in sandstones at the top of the H lithofacies (Fig. 12d) while altered feldspars are surrounded by illite perpendicular coatings (Fig. 12e).

Table 2: Paragenetic sequence proposed for the Villa Monica Formation, Sierra La Juanita, Tandilia

Proccesses	Products
Precipitation and Sedimentation	
• Blue/green algal activity and minor detrital Input	• Boundstones and laminar microbial mats with intercalated siliciclastic deposits
Surficial diagenesis (syndiagenesis)	
• Calcite precipitation	• Microsparite
• Recrystallization	• Macrosparite
• Syngenetic dolomitization	• Dolosparites (tinction with alizarin red)
• Precipitation of biogenic silica	• Opal-A (amorphous SiO_2)
• Silicification at low depth and temperature lower than 70 ℃	• Opal- A→ Opal- CT (trydimite) → Quartz megacrystals
Partial subaereal exposure. (Hiatus)	
• Weathering	• Ghost structure/texture relicts on dolostones
• Dissolution	• Cavities (fenestral porosity). Release of Fe_2O_3, MnO_2 and TiO_2, etc.
• Leaching: eluviation	• Coarser sediment remains
• Deposition (translocation): illuviation	• Clay- skins: cutans (illitic clay infilling)
• Shallowing upward trend in the paleoenvironmental conditions	• Deposition of hetherolitic facies towards the top of the sequence
Several transgressive/regressive cycles with exposure periods	
• Sedimentation /erosion	• Deposition of all the overlying Neoproterozoic units/several weathering products
• Weak epeirogenic movements	• The Neoproterozoic sequences remain subhorizonal
Burial diagenesis of the Neoproterozoic units:	
In the Villa Mónica Fm:	
• Neoformation of minerals	• Silica (secondary overgrowths). (ISII: 1M.). Pyrite (distorting the lamination). Rutile
• Pressure-dissolution by overburden	• Stylolites parallel to bedding, sutural contacts, inter and intraganular dissolution, triaxial junction
Compression (Brazilian movements, 600 Ma)	Faulting, differential blocks movements
Erosion. Topographic height towards the NW (Cambrian)	Peneplanation. Differential removal of the Neoproterozoic sequences toward the NW
Subsidence of another superimposed basin opened to the SE.	Deposition of the Balcarce Formation
Sedimentation, burial diagenesis (Ordovician)	
• Tandilia: Stratigraphic height after the Ordovician	• Exposure
Compression from the SW during middle Permian	Ventania uplift
Telodiagenesis stage in Tandilia (basin inversion):	
In the Villa Mónica Formation:	
• Uplift, erosion, fracturing, folding Introduction of meteoric fluids: neoformation of minerals, lateral presure-dissolution, hydration, dedolomitization, passive precipitation.	• Faults are reactivated and sediments are differentially eliminated. Fluid action on developed fractures: Pyrite oxidation: hematite and diffusion cutans Kaolinite/smectite (ferriargillans and clay skins) Kaolinite hydration→ halloysite Hematite hydration→ goethite Inclined stylolites with ferric oxide relics Ferriargilans and clay skins filled fractures and quartz dissolved and fractured Development of stress cutans (slickensides) and tangential clay coatings Brecciation Continuous and homogeneous calcite rims in well preserved boundstones Calcite precipitation in fractures, cavities and stylolites

DISCUSSION

According to field evidence, mineralogy and the fabric revealed by petrographic and SEM analysis, successive weathering and diagenetic superimposed events have been recognized in the sediments of the Villa Mónica Formation and a paragenetic sequence is proposed (Table 2).

The well-preserved columnar boundstones (Fig. 3) represent the unaltered bedrock, whereas overlying C/S facies with laminar structures and minor intercalated siliciclastics are attributed to microbial activity systematically interrupted by short-lived detrital cycles and which have been extensively weathered. Introduction of illitic epimatrix in the different facies (quartz grains floating in an illitic matrix) is related either to bioturbation, mass flow and soft-sediment deformation in the fabric of marine sandstones (Walker *et al*., 1978). In this case, the phenomenon could be linked to soft-sediment deformation and bioturbation produced by microbial activity.

Algal cementation is one of the most important lithification processes in shallow-water limestone genesis. The lime precipitates of blue-green, green and red algae can be considered as more or less of syngenetic

origin (Larsen and Chilingar, 1979). We interpreted the well-preserved and weathered dolostones found at the Sierra La Juanita, showing cellular/banded, stromatolitic structures and crinkled lamination, to represent the kind of deposits derived from bacteria and blue-green algae activity, according to Schieber (1998).

Calcite derived from microbial activity precipitated as microsparite, which in turn recrystallized to macrosparite. Early diagenetic calcification of microbial deposits promoted the formation of cavities and calcite cement. Some of the voids must have remained open and provided pathways for fluids during later diagenesis (Glumac, 2001).

Trapped sediments between the microbial deposits, represented by detrital sandy or silty quartz, detrital illite ($2M_1$) and micas, were all derived from weathering and erosion of the granitic basement rocks. Flexuration and orientation of the micas parallel to bedding prove their detrital origin. The $1M_1$ polytype is present in minor proportions and is considered to be of burial diagenetic origin.

Staining with Alizarin red shows that all the micro and macrosparite have been transformed into dolomite. The complete process of dolomitization could be interpreted as syngenetic. We assume that dolomitization took place at shallow depth and low temperature (less than 70ºC), according to Girard and Deynoux (1991) and Chafetz and Zhang (1998). Dissolution of the dolostones generated fenestral porosity, which developed under appropriate physiochemical conditions and created cavities.

Paragenetic relations between silicification and dolomitization are extremely useful in helping to establish the timing of silicification. Euhedral crystals of dolomite completely silicified in the carbonates suggest that the dolomitization preceded precipitation of silica as a postdepositional process. Silicification has probably occurred as an early diagenetic process. Opal-A, considered of biogenic origin, recrystallized to opal-CT (trydimite), then to quartz megacrystals (which include opal-CT) which developed in the fenestral cavities.

After the silicification process, subaerial exposure occurred. The sediments must have been eroded to a large extent and extensive weathering occurred with the development of pedogenetic features (e.g., clay illuviation).

Dissolution of the boundstones increased and cavities enlarged and connected with each other. Loose, individual or random aggregates of pyramidal quartz megacrystals, remained *in situ* in the weathered dolostones (C/S facies). Illuviation processes deposited cutans (illitic clay skins: argillans) in the created cavities. As the original rhombohedral dolomite crystals were dissolved, illuviated illitic clays increased in lower horizons.

The ferric oxides may have derived from the dissolution of micas (biotite) contained in higher eluviated horizons, from the replacement of calcium by iron in the dolostones (Larsen and Chilingar, 1979) and from the activity of Cyanobacteria (blue-green algae) cohabiting on microbial film or mat (Dai *et al*., 2004).

Detrital clay beds within the weathered dolostones (C/S facies), are represented by major $2M_1$ illite and subordinate $1M_1$ illite, the latter considered being of diagenetic origin. Some of the clays show no quartz and a face-to-face association of platelets, which were deposited as flocs (card-pack-flocs, Williamson, 1980). They show `swirl patterns´, probably resulting from movements during packing, settling, or soft sediment deformation (Keller, 1978).

Besides, the fines of the overlying heterolithic (H) facies are illitic and bear quartz, which increases upwards. The same illite polytypes are present and considered to be of the same origin as in the previous illitic clays. The upwards increasing trend in quartz content in the (H) facies is consistent with littoral conditions in tidal flats with the development of graded structures due to differential settling from suspension after a flood (Manassero *et al*., 2007).

During burial diagenetic stages, diverse processes took place in the different lithofacies. Neoformation of minerals is represented by silica overgrowths, development of (ISII) with <15% expanded layers ($1M_1$ illite) at the expense of detrital feldspars (perpendicular clay coatings) and of $2M_1$ illite. Other neoformed minerals are rutile, pyrite and minor anatase. Rutile precipitated from titanium oxide contained in the micas, as in many other Neoproterozoic formations of Tandilia (Iñiguez *et al*., 1989) and crystallized as needles (resembling a sagenite-like texture) in the illitic clays and in quartz cement, filling cavities or fractures. Rutile needles are also found in quartz precipitated in pores of the quartzites of the (H) facies. Pressure-solution by overburden originated stylolites parallel to bedding and intergranular (e.g., concave-convex grain contacts) dissolution effects developed in the C/S as well as in the H facies.

After deposition of all the other Neoproterozoic units, a compressive event affecting the Tandilia System (Brazilian cycle, 600 Ma) was responsible for regional faulting, fracturing and differential block elevation (horst and graben structure). Peneplanation presumably took place during the Cambrian (Iñíguez *et al*., 1989).

During early Ordovician, to the SE, subsidence created a new basin, opened to the SE and in which the sediments of the Balcarce Formation were deposited. Tandilia remained as an old topographic height, subsequent to the Ordovician and before the Devonian. Tandilia also represented the NE border of the Claromecó Basin, as suggested by the thinning of all the Palaeozoic deposits of the basin in that direction and the lack of Devonian deposits in the Tandilia mountain range (Lesta and Sylwan, 2005).

During the Permian, uplift of the Ventania System, located 150 km to the SW of Barker, took place (Varela *et al*., 1985; Von Gosen and Buggisch, 1989). According to Zalba *et al*. (2007b) simultaneous compression from the SW occurred in Tandilia. Due to basin inversion, a new stage in the geological history of Tandilia began. During this telodiagenetic stage kaolinite formed due to the introduction of oxidized meteoric fluids related to pyrite oxidation, in the Neoproterozoic Las Aguilas Formation (younger than the Villa Mónica Formation and outcropping 7 km to the east of the Estancia La Siempre Verde), where it is also associated with halloysite, together with diaspore and APS minerals. Based on this evidence it is not unrealistic to suppose that regional telodiagenetic processes developed in the Barker area also affected the studied unit.

It is important to underline that kaolinite has been introduced in the sediments because it is associated with minor smectite in ferriargillans and clay infillings related to a criss-crossing network system of fractures cutting the C/S facies and postdating the illuviation of illitic clay infillings (argillans). It represents the redistribution of neoformed clays in the sediments and in the sedimentary discontinuity between the C/S and the H facies. This would explain the mixture of the kaolinite-halloysite assemblage and/or smectite, with illitic clays which, almost certainly, is the same phenomenon that occurred in most studied clay deposits of Tandilia where this mixture of illite with kaolinite-halloysite is found (Zalba *et al*., 2007b).

Smectite, in variable proportions, is predominately associated with slickensides in reddish clays filling a network system of fractures. The slickensides differ markedly from clay skins, which occur on pedogenetic surfaces resulting from clay translocation. The latter have sharp outer and inner boundaries with distinct extinction patterns and are often finely layered (laminar fabric). The slickensides seem to be aligned preferentially (relative to the stress field) in response to structural deformation (Driese and Foreman, 1992), so they would be of tectonic origin instead of being pedogenetic, which are not oriented and locally form pseudo-anticlines (Driese and Foreman, 1992; Driese *et al*., 1992; Driese and Mora, 1993; Caudill *et al*., 1996).

Smectite may derive from the dolostones which contain the Mg and Fe required for its development as a result of neogenesis or transformation from primary minerals (Worden and Burley, 2003). If smectite had formed earlier than the other clay minerals (as in vertisols) it would have prevented the illuviation (translocation) of illitic clay throughout the weathered boundstones. Furthermore, the presence of smectite-kaolinite-halloysite filling fractures suggests a late origin for these minerals. Smectite was one of the latest minerals to form and must have developed during the telodiagenetic stage. This mineral is also present in other Neoproterozoic units of the Tandilia Basin (e.g., Cerro Negro Formation) and was considered to be of late diagenetic origin (Zalba, 1982).

Cubic crystals of pseudomorphous hematite after pyrite could have formed during this telodiagenetic stage due to oxidizing meteoric fluids. Pyrite was presumably formed during early burial diagenesis, as in other Neoproterozoic deposits of Tandilia (Zalba *et al*., 2007b). Hematite which colored the sediments and is also present as diffusion cutans, needs oxidizing conditions to be formed. Most of the hematite was hydrated to goethite, the latter being a constituent of the ferriargillans. It is present in fractures, in cavities of the weathered boundstones and in the siliciclastics of the C/S facies. Fractures filled with goethite cut the remains of the original boundstones, the ferriargillans and the clay skins in general, demonstrating that goethite post-dated all of them. Petrography shows that goethite grew over smectite and so the first must be younger.

Lateral compressive forces produced pressure-solution effects. Inclined stylolites developed in all the identified facies cutting previous stylolites developed parallel to bedding. They are filled with epimatrix and/or relic ferric oxides (hematite), dissolved and fractured quartz grains and brecciated ferriargillans, which indicate compressive effects.

Folding of the sediments also occurred during telodiagenesis and affected in a different way the lithostratigraphic units because of a different mechanical response of these materials to compressive forces. This folding is clearly appreciated in field and microscopic observations.

Another event attributed to telodiagenesis is the development of kaolinitic epimatrix (tangential clay coatings), clearly connected with fractures, surrounding secondary quartz overgrowths and observed in sandstones of the H facies.

Dedolomitization partially affected the C facies. According to Larsen and Chilingar (1979), dedolomitization can be eogenetic as well as telodiagenetic. In the present case, dedolomitization is recognized by the presence of epitaxial calcite rims on silicified dolomite crystals in the C facies. The rims are even and uniform in thickness. Analysis of the fabric geometry and mineral paragenesis suggest that the rims formed by marginal dedolomitization (Larsen and Chilingar, 1979), attributed to telodiagenetic processes.

Calcification (passive precipitation) also occurred during this telodiagenetic stage. Calcite fills fractures, enlarging them because of its force of crystallization. These fractures cut stylolites, thus postdating them. Calcite also fills large cavities in trapped sediments in the C and C/S facies.

CONCLUSIONS

On the basis of new field and petrographic evidence, three lithofacies overlying the Cuarcitas Inferiores are redefined for the Villa Monica Formation in the study area. (1) Carbonate facies: dolomitized and silicified well preserved stromatolitic boundstones with *in situ* quartz megacrystals and sandy sediments trapped within, (2) Carbonate/Siliciclastic facies: weathered laminar microbial mat deposits with *in situ,* loose quartz megacrystals and intercalated siliciclastic episodes and (3) Heterolithic facies: sandstone-claystone beds with microbial mat activity. Lithofacies 2 and 3 are described for the first time at this locality and also for this lithostratigraphic unit. The heterolithic facies substitute the *Psamopelites* of Poiré and Iñíguez (1984).

The paragenetic sequence of events evidences that carbonate sediments, with cellular and stromatolitic structures, derived from microbial action and intercalated thin, detrital illitic ($2M_1$) greenish clay levels (some of them with no quartz) were deposited under tidal conditions. Illitic clays settled down from suspension and were derived from basement rock erosion.

Syngenetic, surficial processes led to recrystallization of micro-spar to macro-spar, dolomitization, at low depth and temperature (lower than 70°C) and dissolution of the boundstones, release of ferric oxides from the dolostones and from microbial mats and titanium oxides from detrital micas. Cavities formed creating secondary porosity where silica precipitated: opal-A (biogenic), which recrystallized into opal-CT (trydimite) and subsequently, into quartz megacrystals (silicification). Subaerial exposure produced erosion and weathering of the boundstones. Leaching and translocation (illuviation) processes were responsible for the deposition of clay skins or cutans (illitic clay infillings) in cavities and fractures.

The heterolithic facies represent a shallowing upward trend in the paleoenvironmental conditions and the last development of microbial activity in this lithostratigraphic unit. That is why the heterolithic facies are considered part of the biogenerated deposits of the Villa Mónica Formation.

After several recognized transgressive-regressive cycles which led to well known resultant unconformities and weathering products, as well as weak epeirogenic movements throughout the geological history of the basin, a major period of basin subsidence occurred, during which the sediments remained sub-horizontal and experienced burial diagenetic processes. In the Villa Monica Formation these processes were represented by (1) Neoformation of minerals: silica overgrowths on quartz grains; development of ISII with <15% expanded layers ($1M_1$ Illite) at the expense of detrital illite ($2M_1$) and of feldspars (perpendicular coatings); pyrite and rutile/anatase. (2) Pressure-dissolution during burial led to the development of stylolites parallel to bedding, sutured grain contacts, intragranular and intergranular dissolution, with concave-convex contacts between grains.

As exposed in a previous contribution (Zalba *et al*., 2007b) after a complex history of compression which involved faulting, differential block movements and peneplanation, a new phase began. Due to the uplift of Ventania (middle Permian) Tandilia experienced compression from the SW which caused a telodiagenetic stage (basin inversion) with the most important processes in the Villa Mónica Formation involving uplift, erosion, fracturing, folding, introduction of oxidizing meteoric fluids and epimatrix (e.g., tangential clay coatings) and neoformation of minerals in fractures (hematite, kaolinite, smectite), hydration (goethite, halloysite), lateral pressure-dissolution (stress cutans, stylolitization, brecciation), dedolomitization and passive calcite precipitation.

ACKNOWLEDGMENTS

This study was supported by grants from the Comisión de Investigaciones Científicas Provincia de Buenos Aires through the Centro de Tecnología de Recursos Minerales y Cerámica (CETMIC). We thank Lic. María Eugenia Rodríguez (CIC-CETMIC) for assistance in the field.

REFERENCES

Alló, W., E. Domínguez and F. Cravero, 1996. Illite characterization of the La Siempre Verde deposits, Buenos Aires, polytypes indicative of deep diagenesis and slight metamorphism. Proceedings of the 3rd Congress on Mineralogy and Metalogenesis, (CMM'96), La Plata, Argentina, pp: 27-35.

Alló, W., 2001. Illitic ferruginous clay deposits at La Siempre Verde and La Placeres, Barker. Doctoral Thesis, Southern National University, Argentina, pp: 235.

Alló, W. and E. Domínguez, 2002. Diagenetic quartz megacrystals in pelitic facies of the Villa Mónica Formation, Barker, Province of Buenos Aires. Proceedings of the 15th Argentine Geological Conrgess, (AGC'02), El Calafate, Santa Cruz, pp: 383-388.

Brewer, R., 1960. Cutans: Their definition, recognition and interpretation. Eur. J. Soil Sci., 11: 280-292.

Brewer, R., 1976. Fabric and Mineral Analysis of Soils. R.E. Krieger Publishing Co., Huntington, New York, pp: 480.

Caudill, M.R., S.G. Driese and C.I. Mora, 1996. Preservation of a paleo-vertisol and an estimate of Late Mississippian paleoprecipitation. J. Sedimentary Res., 66: 58-70.

Chafetz, H.S. and J. Zhang, 1998. Authigenic euhedral megaquartz crystals in a quaternary dolomite. J. Sedimentary Res., 68: 994-1000.

Cingolani, C.A. and M.G. Bonhomme, 1982. Geochronology of La Tinta Upper Proterozoic sedimentary rocks, Argentina. Precambrian Res., 18: 119-122.

Cingolani, C.A., R. Varela and E. Leone, 1985. The pre-Cenozoic lithostratigraphic units located between La Numancia and Sierra Larga, Sierras Septentrionales of Buenos Aires. Proceedings of the 1st Geological Congresss of Buenos Aires, (GCBA'85), Tandil, pp: 99-100.

Dai, Y., H. Song and J. Shen, 2004. Fossil bacteria in Xuanlong iron ore deposits of Hebei province. Sci. China Ser. D Earth Sci., 47: 347-356.

Driese, S.G. and J.L. Foreman, 1992. Paleopedology and paleoclimatic implications of late ordovician vertic paleosols, Southern Appalachians. J. Sedimentary Petrol., 62: 71-83.

Driese, S.G., C.I. Mora, E. Cotter and J.L. Foreman, 1992. Paleopedology and stable isotope geochemistry of Late Silurian vertic paleosols, Bloomsburg Formation, central Pennsylvania. J. Sedimentary Petrol., 62: 825-841.

Driese, S.G. and C.I. Mora, 1993. Physico-chemical environment of pedogenic carbonate formation in devonian vertic paleosols, central Appalachian, USA. Sedimentology, 40: 199-216.

Dunham, R.J., 1962. Classification of Carbonate Rocks According to Depositional Texture. In: Classification of Carbonate Rocks, Ham, W.E. (Ed.). American Association of Petroleum Geologists, Memoir, USA., pp: 108-121.

Gaucher, C., 2005. Lithostratigraphy, biostratigraphy and geological correlations of the Neoproterozoic-Cambrian craton of the La Plata River (Uruguay and Argentina). Latin Am. J. Sedimentol. Basin Anal., 12: 145-160.

Girard, J.P. and M. Deynoux, 1991. Oxygen isotope study of diagenetic quartz overgrowths from the upper proterozoic quartzites of Western Mali, Taoudeni basin: Implications for conditions of quartz cementation. J. Sedimentary Petrol., 61: 406-418.

Glumac, B., 2001. Influence of early lithification on late diagenesis of microbialites: Insights from δ180 compositions of Upper Cambrian carbonate deposits from the southern Appalachians. PALAIOS, 16: 593-600.

Gómez Peral, L.E., 2008. Petrology and diagenesis of the Precambrian sedimentary units of Olavarría, province of Buenos Aires. Doctoral Thesis, Faculty of Natural Sciences and Museum of La Plata, La Plata University, pp: 278.

Iñíguez, A.M., A. del Valle, D.G. Poiré, L. Spalletti and P.E. Zalba, 1989. Precambrian/LowerPaleozoic Basin of Tandilia, Province of Buenos Aires. In: Argentine Sedimentary Basins, Chebli, G. and L. Spalletti (Eds.). National University of Tucumán, Geological Correlation Superior Institute, Series of Geological Correlation, Argentina, pp: 245-263.

Keller, W.D., 1978. Classification of kaolins exemplified by their texture in scan electron micrographs. Clays Clay Miner., 26: 1-20.

Larsen, G. and G.V. Chilingar, 1979. Diagenesis in Sediments and Sedimentary Rocks. Developments in Sedimentology 25. Elsevier, Amsterdam, pp: 579.

Lesta, P. and C. Sylwan, 2005. The Claromecó Basin. Proceedings of the 6th Congress on Exploration and Development of Hydrocarbons, (CEDH'05), Exploratory Frontier of Argentina, Mar del Plata, 10, pp: 217-231.

Liang, J.J. and F.C. Hawthorne, 1996. Rietveld refinement of micaceous minerals; muscovite- $2M_1$ a comparison with single-crystal structure refinement. Canadian Mineral., 34: 115-122.

López Escobar, K., 2006. Geology and mineralogy of the clay deposits of Don Camilo, La Elvira, Los Cardales and El Ceferino, Sierras Septentrionales of the Province of Buenos Aires, Argentina. Doctoral Thesis, Faculty of Natural Sciences and Museum of La Plata, La Plata University, pp: 269.

López Escobar, K., L. Botto and R. Etcheverry, 2002. Geology and mineralogy of the clay bodies located between the farms La Rosalía, San Eduardo and the Sierra of Los Barrientos, Province of Buenos Aires. Proceedings of the 6th Congress on Mineralogy and Metalogenesis, (CMM'02), Faculty of Exact and Natural Sciences (UBA), Buenos Aires, pp: 239-246.

Manassero, M.J., 1986. Stratigraphy and structure at the eastern sector of the Barker locality, Province of Buenos Aires. Rev. Argentine Geol. Assoc., 41: 375-384.

Manassero, M.J., P.E. Zalba and M. Morosi, 2007. Paleoenvironments and paleogeography of the Villa Mónica Formation, Sierra La Juanita, Tandilia. Proceedings of the 6th Geological and Geophysical Congress of Buenos Aires, Mar del Plata, Argentina, (GGCBAMPA'07), University of Mar del Plata, Argentina, pp: 47-47.

Plançon, A., S.I. Tsipurski and V.A. Drits, 1985. Calculation of intensity distribution in the case of oblique texture electron diffusion. J. Applied Crystallography, 18: 191-196.

Poiré, D.G. and A.M. Iñíguez, 1984. Psamopelites member of the Sierras Bayas Formation, Olavarría, Province of Buenos Aires. Rev. Argentine Geol. Assoc., 39: 276-283.

Poiré, D.G., 1987. Mineralogy and sedimentology of the Sierras Bayas Formation in the septentrional nucleous of the homonymous hills, Olavarría, Province of Buenos Aires. Doctoral Thesis, Faculty of Natural Sciences and Museum of La Plata, La Plata University, pp: 271.

Poiré, D.G., 1993. Stratigraphy of the sedimentary precambrian from Olavarría, Sierras Bayas, Province of Buenos Aires, Argentina. Proceedings of the 12th Argentine Geological Congress and 2nd Congress on Hydrocarbons Exploration, (AGCCHE'93), Mendoza, pp: 1-11.

Poiré, D.G. and L. Spalletti, 2005. The Precambrian-lower Paleozoic sedimentary cover of the Tandilia System. Proceedings of the 16th Argentine Geological Congress, (AGC'05), La Plata, Argentine, pp: 51-68.

Rietveld, H.M., 1969. A profile refinement method for nuclear and magnetic structures. J. Applied Crystallography, 2: 65-71.

Schauer, O. and J. Venier, 1967. Geological observations in the zone of Barker, Sierra of La Tinta, Province of Buenos Aires. Notes of the Commission of Scientific Investigations of the Province of Buenos Aires, La Plata, pp: 1-14.

Schieber, J., 1998. Possible indicators of microbial mat deposits in shales and sandstone: Examples from the Mid-Proterozoic Belt Supergroup, Montana, USA. Sedimentary Geology, 120: 105-124.

Srodoń, J., 1984. X-ray identification of illitic materials. Clays Clay Minerals, 32: 337-349.

Varela, R., L.D. Salda and C. Cingolani, 1985. Structure and geologic composition of the Colorada, Chasicó and Cortapié hills, Sierras Australes of Buenos Aires. Rev. Argentine Geol. Assoc., 40: 254-261.

Von Gosen, W. and W. Buggisch, 1989. Tectonic evolution of the Sierras Australes fold and thrust belt, Buenos Aires Province, Argentina: An outline. Zentralblatt Für Geologie Und Paläontol. Teil, 1: 947-958.

Walker, T.R., B. Waugh and A.J. Crone, 1978. Diagenesis of first-cycle desert alluvium of Cenozoic age, southwestern U.S. and northwestern Mexico. Geol. Soc. Am., 89: 19-32.

Williamson, W.O., 1980. Experiments relevant to the genesis of clay mineral orientation in natural sediments. Clay Minerals, 15: 95-97.

Worden R.H. and S.D. Burley, 2003. Sandstone Diagenesis: the Evolution of Sand to Stone. In: Sandstone Diagenesis: Recent and Ancient, Burley, S.D. and R.H. Worden (Eds.). Reprint Series of the International Association of Sedimentologists, Blackwell Publishing Ltd., New York, pp: 3-44.

Zalba, P.E., 1982. Scan electron micrographs of clay deposits of Buenos Aires Province, Argentina. Proceedings of the International Clay Conference, (ICC'82), Developments in Sedimentology, Elsevier, Bologna-Pavia, Italy, Amsterdam, pp: 513-528.

Zalba, P.E., M.J. Manassero and M. Morosi, 2007a. Weathering and diagenesis in stromatolitic dolostones, Villa Mónica Formation (Precambrian), Sierra La Juanita, Tandilia. Proceedings of the 6th Geological and Geophysical Congress of Buenos Aires, (GGCB'07), University of Mar del Plata, pp: 46-46.

Zalba, P.E., M.J. Manassero, E. Laverret, D. Beaufort, A. Meunier, M. Morosi and L. Segovia, 2007b. Middle Permian telodiagenetic processes in Neoproterozoic sequences, Tandilia System Argentina. J. Sedimentary Res., 77: 525-538.